Satellites and large doping and temperature dependence of electronic properties in hole-doped BaFe$_2$As$_2$ – Supplementary Information

Philipp Werner,[1,2] Michele Casula,[3] Takashi Miyake,[4,5,6] Ferdi Aryasetiawan,[7,8] Andrew J. Millis,[9] and Silke Biermann[10,5]

[1]*Department of Physics, University of Fribourg, 1700 Fribourg, Switzerland*
[2]*Theoretische Physik, ETH Zurich, 8093 Zürich, Switzerland*
[3]*CNRS and Institut de Minéralogie et de Physique des Milieux condensés,*
case 115, 4 place Jussieu, 75252, Paris cedex 05, France
[4]*Nanosystem Research Institute (NRI) RICS, AIST, Tsukuba, Ibaraki 305-8568, Japan*
[5]*Japan Science and Technology Agency, CREST*
[6]*Japan Science and Technology Agency, TRIP*
[7]*Department of Physics, Mathematical Physics, Lund University, Sölvegatan 14A, 223 62 Lund, Sweden*
[8]*Graduate School of Advanced Integration Science, Chiba University, Chiba 263-8522, Japan*
[9]*Department of Physics, Columbia University, 538 West 120th Street, New York, New York 10027, USA*
[10]*Centre de Physique Théorique, Ecole Polytechnique, CNRS, 91128 Palaiseau, France.*

These supplementary notes describe the methods used in our ab-initio simulation of BaFe$_2$As$_2$ with dynamically screened interactions.

A. Frequency dependent interaction from constrained RPA

In the constrained RPA (cRPA) method[1,2] we first define a one-particle subspace $\{\psi_d\}$ of the low-energy space, which we call the "d subspace", and label the rest of the Hilbert space by $\{\psi_r\}$ ("r subspace"). In the present case, we choose 10 states having strong Fe-3d character as the d subspace (see Fig. 1). We define $P_d(\mathbf{r},\mathbf{r}';\omega)$ to be the polarization within
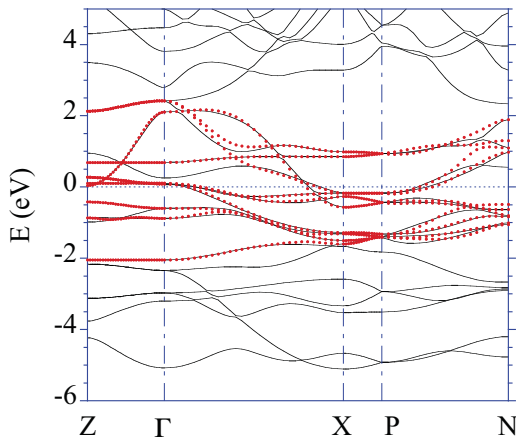

FIG. 1: Electronic band structure of BaFe$_2$As$_2$. The black lines show the LDA band structure, whereas the red dots are interpolated bands in the d subspace obtained using the maximally localized Wannier function procedure.

the d subspace and $P(\mathbf{r},\mathbf{r}';\omega)$ as the total polarization. The rest of the polarization $P_r = P - P_d$ is not the same as the polarization of the r subspace alone because it contains polarization arising from transitions between the d and r subspaces. The physical idea behind the cRPA method is that the Hubbard U, defined as an effective interaction between electrons

in the low-energy effective theory, must be such that when it is screened by the polarization of the low-energy states, it should be equal to the fully screened interaction W of the whole system. We thus define the partially screened Coulomb interaction $W_r(\mathbf{r},\mathbf{r}';\omega)$ by

$$W_r(\omega) = [1 - V P_r(\omega)]^{-1} V, \qquad (1)$$

with V denoting the bare Coulomb interaction. The d states are entangled with others in the present system. In order to distinguish between P_d and P_r, we apply a disentangling procedure[3].

The Hamiltonian for our DMFT calculations contains the ten bands around the Fermi level with dominantly Fe-d character and also the six bands (located at -6 to -2 eV) mainly coming from the As-p bands. The Fe-d orbitals are treated as correlated, whereas the As-p orbitals are assumed to be non-interacting.

The action, equation (4) of the main text, requires the bare unscreened parameters $V_{mm'}$ and $J_{mm'}$, which are obtained as onsite matrix elements $V_{mm'} = \langle mm'|V|mm'\rangle$ and $J_{mm'} = \langle mm'|V|m'm\rangle$ of the bare Coulomb interaction in the maximally localized Wannier functions (MLWF)[4,5] m, m' for the Fe-d orbitals. The action also requires the screening U_{retarded} of the monopole term in the interaction (last line in equation (4)). This is obtained from the average over orbital entries of the matrix $\langle mm'|W_r|mm'\rangle$ as $U_{\text{retarded}} = \frac{1}{5}\sum_m \langle mm|W_r - V|mm\rangle$.

The frequency dependence of the partially screened interaction, averaged over diagonal elements, $U(\omega) = \frac{1}{5}\sum_m \langle mm|W_r|mm\rangle$ is plotted in Fig. 1 of the main text. To illustrate the difference to the fully screened interaction $W(\omega) = [1 - V P(\omega)]^{-1}V$, we plot the analogous diagonal matrix element average $W(\omega)$ in Fig. 2. Note that Re$U(\omega = 0) = 3.61$ eV, while Re$W(\omega = 0) = 0.975$ eV. We emphasize that the physically relevant quantity is the one in Fig. 1 of the main text; Fig. 2 is only for comparison.

In more familiar notation, our procedure corresponds to including screening effects on the charging energy "U", while leaving the higher multipole interaction at their unscreened value. In the cRPA the screening effects on J are very small ($\sim 15 \%$ variation between high- and low-frequency value).

Our parameters correspond to the value $J = 0.68$eV, as obtained from the average over the off-diagonal matrix elements of $J_{mm'}$. In agreement with previous studies on other iron pnictides[10,11] we find that the simulation results depend sensitively on the value of the Hund's coupling J.

In practice, our dynamical mean field procedure for treating the screening effects amounts to employing a Hamiltonian with an instantaneous interaction, equal to the screened interaction and with hybridisation events dressed by a Lang-Firsov factor which accounts for the dynamics of screening. Because we screen only the monopole interactions, the "screened interactions" are constructed as follows: we use the bare value of J ($= 0.68$ eV), and the Slater integral F_0 ($= 2.84$ eV) which is such that the partially screened value of the intraorbital interaction reproduces the orbital average over the cRPA values. We then calculate the symmetrized version of the interaction matrices following the standard Slater parametrization as e.g. described in Ref. 8. To be specific, we write the interaction as matrices for same and opposite spin in orbital space, with the order of the orbitals as follows: $xy, yz, z^2, zx, x^2 - y^2$.

$$U_{mn}^{\sigma\bar{\sigma}} = \begin{pmatrix} 3.61 & 2.57 & 2.42 & 2.57 & 3.03 \\ 2.57 & 3.61 & 2.88 & 2.57 & 2.57 \\ 2.42 & 2.88 & 3.61 & 2.88 & 2.42 \\ 2.57 & 2.57 & 2.88 & 3.61 & 2.57 \\ 3.03 & 2.57 & 2.42 & 2.57 & 3.61 \end{pmatrix}, \quad (2)$$

$$U_{mn}^{\sigma\sigma} = \begin{pmatrix} 0.00 & 2.05 & 1.82 & 2.05 & 2.74 \\ 2.05 & 0.00 & 2.51 & 2.05 & 2.05 \\ 1.82 & 2.51 & 0.00 & 2.51 & 1.82 \\ 2.05 & 2.05 & 2.51 & 0.00 & 2.05 \\ 2.74 & 2.05 & 1.82 & 2.05 & 0.00 \end{pmatrix}. \quad (3)$$

For comparison, we also give the matrices obtained from the cRPA calculation at vanishing frequency:

$$(U_{cRPA})_{mn}^{\sigma\bar{\sigma}} = \begin{pmatrix} 3.80 & 2.42 & 2.31 & 2.42 & 2.86 \\ 2.42 & 3.56 & 2.73 & 2.34 & 2.33 \\ 2.31 & 2.73 & 3.73 & 2.73 & 2.22 \\ 2.42 & 2.34 & 2.73 & 3.56 & 2.33 \\ 2.86 & 2.33 & 2.22 & 2.33 & 3.43 \end{pmatrix}, \quad (4)$$

$$(U_{cRPA})_{mn}^{\sigma\sigma} = \begin{pmatrix} 0.00 & 1.79 & 1.59 & 1.79 & 2.49 \\ 1.79 & 0.00 & 2.27 & 1.76 & 1.72 \\ 1.59 & 2.27 & 0.00 & 2.27 & 1.54 \\ 1.79 & 1.76 & 2.27 & 0.00 & 1.72 \\ 2.49 & 1.72 & 1.54 & 1.72 & 0.00 \end{pmatrix}. \quad (5)$$

B. Dynamical mean field (DMFT) calculation with frequency dependent interaction

The Coulomb matrix elements (2) and (3), their frequency dendence (encoded by Im$U(\omega)$) and the Hamiltonian matrix H_k for the p and d bands in the Wannier basis are the input of the DMFT calculation. DMFT neglects the momentum dependence of the self-energy and replaces the lattice problem by a 5-orbital impurity model with frequency dependent local interactions, and a self-consistency procedure (involving H_k), which fixes the hybridization functions[9]. Since the LDA
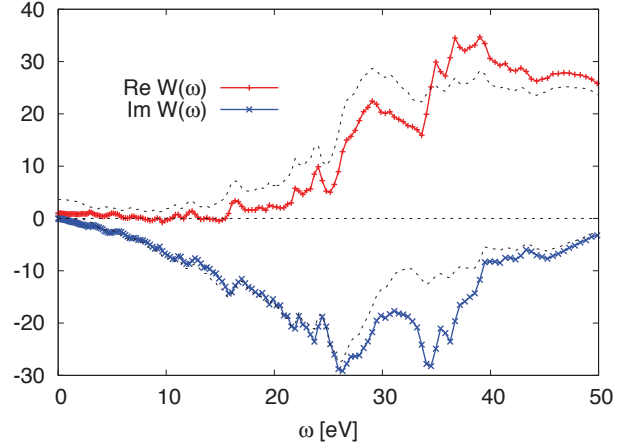
FIG. 2: Frequency dependence of the fully screened Coulomb interaction $W(\omega)$ for $BaFe_2As_2$, obtained as the average over the diagonal matrix elements within the maximally localized Wannier basis: $W(\omega) = \frac{1}{5}\sum_m \langle mm|W|mm\rangle$. The dashed lines show the result for the partially screened Coulomb interaction $U(\omega) = \frac{1}{5}\sum_m \langle mm|W_r|mm\rangle$.

bandstructure (H_k) already captures some correlation effects in the d-orbitals, we modify the self-energy Σ_d by an orbital independent shift (double-counting correction) of

$$E_{DC} = F_0(n_d - 1/2) - J(n_d/2 - 1/2), \quad (6)$$

with n_d the self-consistently computed number of d electrons. This double counting was found in Ref. 12 to yield the best agreement between charge-selfconsistent and non-selfconsistent calculations. Note that the static value of the interaction appears in E_{DC}. This is because the addition of bosonic modes in a dynamically screened model requires the introduction of additional double counting terms for these modes, which eliminate the bare interaction from the double counting formula.

The new feature, compared to previous LDA+DMFT simulations, is the treatment of the full frequency dependence of the interaction. We employ the method developed in Refs. 13,14, which is based on the hybridization expansion approach[15]. This technique can be easily generalized to multi-orbital systems. We define the bosonic factor $b(\omega', \tau) = \cosh\left[(\tau - \frac{\beta}{2})\omega'\right]/\sinh\left[\frac{\omega'\beta}{2}\right]$ and the function (valid for $0 \le \tau \le \beta$)

$$K(\tau) = \int_0^\infty \frac{d\omega'}{\pi} \frac{\text{Im}U_{\text{retarded}}(\omega')}{\omega'^2}[b(\omega', \tau) - b(\omega', 0)], \quad (7)$$

which corresponds to the twice integrated nonlocal interaction. The frequency dependence of U then enters the hybridization expansion calculation in the form of a non-local interaction between each pair of creation and/or annihilation operators (irrespective of orbital) of the form $w_{ij} = \exp[s_i s_j K(\tau_i - \tau_j)]$, where $\tau_i > \tau_j$ are the positions of the two hybridization events on the imaginary time interval and $s = 1$ for creation operators and -1 for annihilation operators. Apart from these modifications, the impurity calculation

proceeds as usual (with the static value of U (equations $(2, 3)$) for the evaluation of the interaction contribution to the Monte Carlo weight), via random insertions and removals of pairs of hybridization operators. For models with density-density interaction, this method is highly efficient. At the lowest temperature, $T = 145$ K, we used about 10 CPU hours per iteration.

C. Analytical continuation

The DMFT calculation yields an imaginary-time Green function which contains all the dynamic features encoded in the retarded interaction $U(\omega)$. However, to analyze the effects of the retarded interaction on the spectral function, an inversion procedure is required which allows us to go from the imaginary time to the real time domain. The stochastic noise in the CTQMC data makes this problem extremely difficult for standard Maximum entropy methods if one aims at resolving intermediate-to-high energy features like the satellites discussed in the main text. In Ref. 16, a new analytical continuation procedure has been proposed which is based on the exact atomic limit properties of quantum impurity problems with retarded interactions. In that limit, the exact Green function becomes the product of a purely static (local in time) interacting part, $G_{\text{static}}(\tau)$, and the factor $B(\tau) = \exp[-K(\tau)]$ with bosonic symmetry containing the full retarded tail of the interaction U. G_{static} and B are analytically known, and B is responsible for both the low-energy renormalization of the Green function, and the satellites resulting from the screening processeses embedded in U. The information encoded in the B factor gives the correct asymptotics and intermediate-

to-high energy properties even away from the atomic limit, as the hybridization affects mainly the low-energy part of the spectral function.

Motivated by these considerations we introduce an auxiliary Green function $G_{\text{auxiliary}}$ satisfying

$$G(\tau) = G_{\text{auxiliary}}(\tau)B(\tau). \tag{8}$$

$G_{\text{auxiliary}}$ describes mainly the low-energy features of the full Green function, thanks to the energy scale separation in the spectrum. Therefore, the standard maximum entropy method can be applied reliably to compute the spectral function ρ_{aux} of $G_{\text{auxiliary}}$, while ρ_B - the spectral representation of the Bose factor B - can be obtained via the numerical integration of equation (7) at any desired accuracy. The full spectral function is obtained from the integral

$$\rho(\omega) = \int_{-\infty}^{\infty} d\epsilon \, \rho_B(\epsilon) \frac{1 + e^{-\beta\omega}}{(1 + e^{\beta(\epsilon-\omega)})(1 - e^{-\beta\epsilon})} \rho_{\text{aux}}(\omega - \epsilon). \tag{9}$$

At zero temperature, equation (9) reduces to the convolution of ρ_B and ρ_{aux}.

The bosonic spectral function ρ_B for $BaFe_2As_2$ is shown in Fig. 1 of the main text. It essentially inherits the structures from $\text{Im}U(\omega)/\omega^2$. If $\rho_{\text{aux}}(\omega)$ has a sharp peak at $\omega \approx 0$, this convolution will produce a satellite at each of the energies corresponding to sharp features in ρ_B.

To analytically continue the self-energy, $\Sigma(i\omega_n)$, we define an effective Green function $G^{\Sigma}(i\omega_n) = [i\omega_n - \mu_{\text{eff}} - \Sigma(i\omega_n)]^{-1}$ and apply the above procedure to $G^{\Sigma}(i\omega_n)$. From its spectral function $\rho^{\Sigma}(\omega)$, the calculation of $\Sigma(\omega)$ follows straightforwardly through the Kramers-Kronig relations.

[1] Aryasetiawan, F., Imada, M., Georges, A., Kotliar, G., Biermann, S. & Lichtenstein, A. I. Frequency-dependent local interactions and low-energy effective models from electronic structure calculations. *Phys. Rev. B* **70**, 195104 (2004).

[2] Aryasetiawan, F., Karlsson, K., Jepsen, O., & Schoenberger, U. Calculations of Hubbard U from first-principles. *Phys. Rev. B* **74**, 125106 (2006).

[3] Miyake, T., Aryasetiawan, F., & Imada, M. Ab initio procedure for constructing effective models of correlated materials with entangled band structure *Phys. Rev. B* **80**, 155134 (2009).

[4] Marzari, N. & Vanderbilt, D. Maximally localized generalized Wannier functions for composite energy bands. *Phys. Rev. B* **56**, 12847-12865 (1997).

[5] Souza, I., Marzari, N. & Vanderbilt, D. Maximally localized Wannier functions for entangled energy bands. *Phys. Rev. B* **65**, 035109 (2001).

[6] Miyake, T. & Aryasetiasan, F. Screened Coulomb interaction in the maximally localized Wannier basis. *Phys. Rev. B* **77**, 085122 (2008).

[7] Aichhorn, M., *et al.* Dynamical mean-field theory within an augmented plane-wave framework: Assessing electronic correlations in the iron pnictide LaFeAsO *Phys. Rev. B* **80**, 085101 (2009).

[8] Lichtenstein, A. I., Anisimov, V. I., & Zaanen, J. Density-functional theory and strong interactions: Orbital ordering in Mott-Hubbard insulators. *Phys. Rev. B* **52**, R5467-5470 (1995).

[9] Kotliar, G. *et al.*, Electronic structure calculations with dynamical mean-field theory. *Rev. Mod. Phys.* **78**, 865-951 (2006).

[10] Haule K, & Kotliar, G. Coherenceincoherence crossover in the normal state of iron oxypnictides and importance of Hund's rule coupling. *New J. Phys.* **11** 025021 (2009).

[11] Ishida, H., & Liebsch, A. Fermi-liquid, non-Fermi-liquid, and Mott phases in iron pnictides and cuprates. *Phys. Rev. B* **81**, 054513 (2010).

[12] Aichhorn, M., Pourovskii, L., & Georges, A. Importance of electronic correlations for structural and magnetic properties of the iron pnictide superconductor LaFeAsO. Preprint at http://arxiv.org/abs/1104.4361.

[13] Werner, P. & A. J. Millis, A. J. Efficient DMFT-simulation of the Holstein-Hubbard Model. *Phys. Rev. Lett.* **99**, 146404 (2007).

[14] Werner, P. & Millis, A. J. Dynamical Screening in Correlated Electron Materials. *Phys. Rev. Lett.* **104**, 146401 (2010).

[15] Werner, P., Comanac, A., De' Medici, L., Troyer, M. & Millis, A. J. A continuous-time solver for quantum impurity models. *Phys. Rev. Lett.* **97**, 076405 (2006).

[16] Casula, M., Rubtsov, A. & Biermann, S. Dynamic screening effects in correlated systems: a Greens function ansatz for the dynamical mean eld theory approach. *Phys. Rev. B* **85**, 035115 (2012).